

## LES and Experimental investigation of Diesel sprays

Chawki Habchi\* and Gilles Bruneaux  
IFPEN, 1&4, avenue Bois-préau, 92852 Rueil-Malmaison, France  
[Chawki.Habchi@ifpen.fr](mailto:Chawki.Habchi@ifpen.fr) and [Gilles.Bruneaux@ifpen.fr](mailto:Gilles.Bruneaux@ifpen.fr)

### Abstract

In this paper, a Diesel spray has been investigated experimentally and numerically in order to improve the understanding of transient processes of short injection typically used in multi-injection strategies of internal combustion engine. The spray was observed experimentally in a high pressure high temperature cell that reproduces the thermodynamic conditions which exist in the combustion chamber of a Diesel engine during injection using a pre-combustion technique. A single-hole injector was mounted within the top face of the cell and the spray was injected at the following operating conditions:  $P_{inj} = 120$  MPa,  $T_{gas} = 900$  K and  $P_{gas} = 6.7$  MPa. The injected fuel was a mixture of 70% vol n-decane and 30% vol 1-methylnaphtalene representative of a standard diesel. Planar Laser-induced Fluorescence (PLIF) was used to obtain two dimensional fields of fuel mass concentration. A normalization method based on the determination of the total injected mass was used to derive quantitative information from the fluorescence imaging. Also, 50 single-shot images of the vapor jet were acquired in order to allow statistical analysis.

Large Eddy Simulation (LES) numerical approach has been used in order to investigate single-shot transient processes and averaged results. First, a new Lagrangian injection model is suggested in order to improve the initial formation of dense sprays in LES simulations. Different LES simulations have been carried out using a Lagrangian approach including recently developed models in the AVBP code, for instance, the energy Spectrum Analogy Breakup (SAB) model for the droplets breakup. Five test cases were computed. For each case, a series of 15 or 30 LES was calculated by setting different seeds for random sampling of the injected blobs. These numerical investigations have shown that accurate initial injection boundary conditions (injection flow rate, turbulence level, effective orifice section due to cavitation) and numerical sub-models (injection model, SGS turbulence model) are the most important factors for the prediction of Diesel sprays. In addition, it has been shown that more than 30 LES simulations are needed in order to obtain converged numerical results. In this case, a satisfactory quantitative agreement has been obtained between the numerical results and the experiments, in terms of mass density, both in the averaged images and for the axial and radial profiles.

---

### Introduction

The injection of liquid fuels in recent internal combustion engines is performed using high pressure (HP) injection systems. Injectors with multi-holes nozzle are often used. However, other technologies of injectors using external valve nozzles are also employed, for example, in gasoline direct injection (GDI) engines. Such HP injectors lead to a gradual atomization of liquid jet in a cloud of fine droplets usually called spray. This process, called primary atomization, takes place in a zone near the injector exit. This zone is governed by a set of complex physical phenomena with very small characteristic scales. The structure of the dense zone has been investigated experimentally using different sophisticated optical techniques [1] [2]. On the numerical side, different approaches have been used to investigate primary atomization of liquid jet [3] [4] [5] [6] [7]. However, the underlying physical processes are currently not completely identified nor well understood. One can imagine that the dense zone includes a liquid core (or sheet) and different ligaments and droplets sizes in a highly turbulent gas flow. For high Reynolds number conditions, the liquid flow itself in the orifices is turbulent and may include cavitation or flash boiling bubbles that are known to enhance the primary atomization. The dense zone is presently not directly calculated in CFD simulations of two-phase engines because the Eulerian-Lagrangian (EL) approach cannot describe properly the primary atomization and the Eulerian-Eulerian (EE) approach is still a work in progress [8] [9] [10]. Different models of injection are proposed in the literature for the EL and EE approaches. These models are based on different ideas that mimic the physics of primary atomization in the dense area of the jet. For the computations of Diesel sprays, the 'blob' injection model of Reitz [11] is one of the most used in the literature when the primary atomization is taken into account [12] [13] [14] [15]. The injected 'blobs' have an initial diameter close to the injector orifice. In addition, computational cell sizes, which are larger than the orifice diameter, are typically employed in order to keep the liquid volume fraction small and ensure numerical stability. However, these grid sizes are not adequate to resolve the jet shear layer and gas entrainment. Three

---

\* Corresponding author: [Chawki.Habchi@ifpen.fr](mailto:Chawki.Habchi@ifpen.fr)

alternative approaches have recently been tested by Abraham and Pickett [16]. First, they injected smaller droplets than the ‘blobs’ using an initial size distribution with a relatively small SMD (Sauter mean diameter). In addition the droplets were injected with a specified cone angle from a source line on the orifice axis. The length of this source line is another parameter of the model taken equal to half the experimental liquid penetration length. The two other alternative approaches have been originally developed by Abraham [17] in order to be able to employ adequate grid resolutions in numerical computation of transient jets. In these models, droplets are not explicitly modeled. The first model is the gas jet model which assumes that turbulent (gas or liquid) jets of the same mass and momentum flow rates have similar penetration and spreading. This assumption makes the diameter of the orifice for the gas jet much larger than the actual orifice. In the second model called VLS, it is assumed that there is a core of liquid originating from the injector orifice which is a source of vapor fuel mass, momentum and energy [18]. Another alternative approach has been recently employed by Martinez et al. [19] and Sanjose et al. [20] for EE-LES of Diesel sprays and aero-engine hollow-cone sprays, respectively. The method is to shift the injection location from the orifice area (where the liquid flow cannot be computed by the mesoscopic-EE approach [21]) to a surface,  $S_{offset}$  located at the tip of the dense liquid jet zone where the liquid is assumed already as droplets. This shift was assumed equal to ten orifice diameters by Martinez et al. [19] for single-hole Diesel spray simulations. In addition, they used Gaussian profiles for the injection velocity and volume fraction at the offset surface,  $S_{offset}$ . Furthermore, by specifying both the velocity of the liquid and gas on the offset section, their model *DITurBC* (Downstream Inflow Turbulent Boundary Conditions model) seems able to properly simulate the initial entrainment of gas by the liquid jet. Although most of these models have given satisfactory numerical results, they use concepts rather far from the physics of the injection. Indeed, among the significant simplifications, most of them ignore the dense region of the jet although the origin of its development. The purpose of this paper is to propose models for liquid injection that are closer to the physics of the injection as part of the Lagrangian approach. Although one can find in the literature a large number of articles on liquid sprays, there is little experimental data for a precise validation of two-phase flow models. In this work, the evaluation of the performance of the new models is carried out by comparing the numerical results with a dedicated experiment having a well controlled ambient conditions similar to those of a Diesel engine [22] [23]. In this experiment, fuel concentration maps are obtained by a normalized Laser Induced Fluorescence technique. This article is organized as follows. First, a new Lagrangian model for the initial formation of dense sprays in LES simulations is suggested. Next, the experimental technique is described along with the results obtained in the conditions similar to internal combustion engines. Then, different LES simulations have been carried out and compared to the previously acquired experiments. Finally, conclusions and future work are highlighted.

## Numerical injection Model

The main idea of the injection model suggested in this work is to define, at the nozzle exit, a Dense Volume of Injection (DVI) region where the two-phase flow is completely specified in terms of volume fraction, velocity and turbulence for both liquid and gas phases. The liquid in the DVI region is assumed already atomized into blobs of different shapes and characteristic sizes. The liquid is injected randomly in the DVI region using a specified blobs size distribution. The idea is to inject blobs more frequently in the liquid core zone using a Gaussian distribution. Indeed, Yue et al. [1] investigated diesel fuel spray characteristics using X-ray absorption and they reported that the radial mass distribution of the fuel can be well described by a Gaussian distribution near the nozzle. This observation is corroborated by the LDV velocity measurements of Chaves et al. [24] using a single-hole nozzle. Indeed, the experimental velocity profiles obtained at a distance  $x/d_0 = 10$  from the nozzle, with  $d_0$  the diameter of the orifice, have a shape close to a Gaussian distribution. Hence, the Gaussian distribution is also applied to the injection velocity. In addition, the injection velocity is applied both to the injected blobs and to the gas velocity inside the DVI region in which the mesh is assumed sufficiently refined. Generally speaking, the suggested DVI method may be applied to any nozzle configuration. But in this work, the DVI method is applied to the nozzles most commonly used, namely those with holes such as in Diesel injectors.

## DVI model for Single-hole nozzles

In the case of a single-hole nozzle, the DVI region is assumed in the form of a truncated cone (Figure 1). This cone is limited, at the top, by the exit section of the orifice and at the bottom by a circular area defined by two user data, the cone angle,  $\theta$  and the length of the intact liquid core,  $L_{intact}$ . The liquid volume fraction and the injection velocity are specified using 3D Gaussian distributions. As already mentioned, the liquid is injected randomly in the DVI region using a specified size distribution. To determine the position of injection of every blob in the DVI region, three random numbers,  $RN$  are used. Two of them are randomly chosen in a uniform distribution between 0 and 1.  $RN_1$  determines the axial coordinate,  $z_{inj}$  of the injection section (Figure 2).

$$z_{inj} = L_{intact} RN_1 \quad (1)$$

If the  $RN_1$  value is 0,  $z_{inj}$  is equal to 0 and the blob is injected in a point of the hole exit section. If the  $RN_1$  value is 1,  $z_{inj}$  is equal to  $L_{intact}$  and the blob is injected in a point of the offset section,  $S_{offset}$ . The second random number,  $RN_2$  determines the direction of injection,  $\phi$  between 0 and  $2\pi$ . Finally, the last random number,  $RN_3$  is chosen in a Gaussian distribution in order to determine the initial radial position of injection,  $r_{inj}$ :

$$r_{inj} = r_{prof} \frac{erf^{-1}(RN_3)}{2} \quad (2)$$

where  $erf$  is the error function and  $r_{prof}$  is the radius of the current injection section which may be readily computed using  $d_0$ ,  $z_{inj}$  and the given spray-cone angle  $\theta$  (see Figure 2). Next, the mean intensity of the injection velocity,  $u_{inj}$  is computed using the same random number,  $RN_3$  as follows:

$$u_{inj} = V_{FR} \left[ 1 - \frac{erf^{-1}(RN_3)}{2} \right] \quad \text{with} \quad V_{FR} = \frac{Cd_{vit}}{\alpha_l} \frac{M_{dot}}{\rho_l A_0} \quad (3)$$

where  $V_{FR}$  is the injection velocity which is computed from the instantaneous injection rate,  $M_{dot}$ .  $\rho_l$  is the liquid mass density,  $A_0$  is the hole exit area,  $\alpha_l$  is the liquid volume fraction at hole exit area and  $Cd_{vit}$  is a discharge velocity coefficient. Then, it becomes possible to compute the three components of the velocity for each injected blobs,  $u_{b,i}$  ( $i=1,3$ ) by:

$$u_{b,i} = u_{inj} \left[ \frac{n_i + tg\left(\frac{\theta}{2}\right)t_i}{1 + tg\left(\frac{\theta}{2}\right)} + (2RN_i - 1)V_{rms} \right] \quad (4)$$

where  $n_i$  and  $t_i$  are, respectively the components of the normal and radial unit vectors depicted in Figure 2. The second term in Equation (4) is the turbulent component of the injection velocity,  $u'_{inj}$ . It is defined for each component  $i$  using a given dimensionless velocity fluctuation,  $V_{rms}$ , and three supplementary random numbers ( $RN_i$ ,  $i=1, 3$ ), as follows:

$$u'_{inj,i} = u_{inj} (2RN_i - 1)V_{rms} \quad (5)$$

The opening and closing of the needle are also taken into account in the DVI model. During these transient periods (denoted  $dt_{open}$  and  $dt_{close}$  in Table 2), the injection velocity is assumed to vary linearly with time, between zero and its  $V_{FR}$  steady value given by Equation (3), as follows:

$$\begin{aligned} V_{FR,open} &= V_{FR} \frac{t}{dt_{open}} & t \leq dt_{open} \\ V_{FR,close} &= V_{FR} \frac{(T_{inj} - t)}{dt_{close}} & t \geq (T_{inj} - dt_{close}) \end{aligned} \quad (6)$$

Finally, the gas velocity,  $u_g$  at the nearest node to the initial position of the injection ( $z_{inj}, r_{inj}$ ) is specified as follows:

$$u_{g,i} = F_{glis} u_{b,i} \quad (7)$$

Indeed, the gas velocity in the DVI region is assumed proportional to the blobs injection velocity in order to ensure a correct initial gas entrainment by the liquid jet. The entrainment factor, denoted  $F_{glis}$ , is among the parameters of the DVI model (see Table 2). Moreover, a sufficiently refined mesh is required for this direct-coupling between the gas and the liquid blobs. Finally, it is important to note that a standard two-way coupling is applied to the droplet/blobs in the DVI region, except the gas momentum for which Equation (7) superimposes a different value in order to improve gas entrainment near the nozzle.

## Experimental configuration

### High Pressure Cell

The experimental results have been performed in a high-pressure, high-temperature cell which enables the study of spray behaviour under thermodynamic conditions similar to those of a Diesel engine at specified injection timing. The injector is mounted within the top face of the cell. In addition, five sapphire windows with 80mm diameter and 20mm thickness can be mounted on the remaining faces of the cell. Prior to performing the experiments, the gases within the cell are heated and pressurized to reproduce typical in-engine conditions by a

pre-combustion technique similar to that described in [25]. The start of injection (SOI) takes place at a specified time after pre-combustion ignition. The SOI time is determined so that injection takes place when the temperature and pressure in the cell have reached the desired values. The pre-combustion gas mixture can be computed to consume a certain quantity of the oxygen initially introduced in the cell. As a result, experiments can be performed at various oxygen concentrations. The experiments used in this paper have been performed with 0% oxygen. In addition, the case with ambient temperature of 900K and ambient density of  $25\text{kg/m}^3$  was selected to enable pure vaporization investigations. Further details concerning the cell and its operation can be found in previous publications, for instance [26].

### **Injection system**

A second generation Bosch common-rail injector was mounted in the metal top-port, directing a spray downwards into the center of the chamber. The nozzle used through all experimental investigations in this work was a single-hole nozzle with an orifice diameter of 0.2 mm. Injection pressure was supplied by a CP3 Bosch pump entrained by an electric motor.

### **Measurement technique**

The vapor phase of the spray was visualized by Laser Induced Exciplex Fluorescence (LIEF). Details concerning the principle of the technique are available in refs. [23] and [27]. Usually the exciplex technique is used to distinguish the fluorescence emanating from the liquid and vapor phases. However in the present study, the investigation is focused on the vapor phase of the spray when no liquid phase is present. We still decided to use the exciplex technique although its main feature will not be used, in order to profit from the normalization method that was developed in [28] for the quantitative analysis of the vapor phase. The experimental setup for fuel vapor visualization by LIEF is presented in Figure 4. TMPD tracer was added (0.5% by mass) to the fuel mixture consisting of 70% n-decane and 30% 1-methylnaphthalene, and its fluorescence was excited with a frequency-tripled Nd:YAG laser at 355nm. The laser beam is transformed into a laser sheet passing through the injector axis using a cylindrical lens and a spherical lens. This laser sheet has a width of 0.5mm and a height 70mm. A 12bit intensified CCD camera coupled to a 80mm, f/1.4 objective was used to record fluorescence signal. In order to spectrally isolate the LIEF signal it was necessary to use appropriate optical filters (Band Pass 390nm interference filter, FWHM 10nm). Although some degree of spectral separation can be achieved to discriminate between the liquid and vapor phase fluorescence signals [27], in practical the signal intensity from the exciplex fluorescence corresponding to the liquid phase is generally visible when collecting the TMPD fluorescence corresponding to the vapor phase. This is due to the high fluorescence yield of exciplex fluorescence in the dense liquid spray. To avoid possible data misinterpretation, a mask was used in the presence of liquid droplet (i.e. during injection) to block the part of the laser sheet illuminating the liquid part of the spray. The position of the mask was determined by Mie scattering imaging. The fluorescence intensity images were processed according to the following procedure: a first order numerical filter was first applied to reduce the effect of intensifier noise, then the images were corrected by the laser intensity profile, and also corrected for beam steering effects. Finally, the image intensity were normalized to obtain fuel mass concentration fields as described in [28]. This normalization method takes into account the three-dimensional structure of the vapor plume and uses the known injected mass at each instant to estimate the local fuel mass concentration.

### **LES Diesel spray computations**

The DVI model suggested in this paper has been implemented in the LES AVBP code. The main characteristics of this solver may be found in [29] for instance. Particularly, the AVBP solver includes the droplets secondary breakup SAB model, recently published by the authors [30]. The DVI model is applied to the Bosch common-rail injector which has been investigated experimentally. Let's recall that the database includes maps of fuel mass density obtained by PLIF optical diagnostic technique. Instantaneous and the average results of 50 successive injections have been investigated in this work. The condition investigated is referred T9P12 and corresponds to a short injection (actual duration =  $340\mu\text{s}$ ) in a high pressure cell (67bar) and a temperature of 900K with a single-hole injector operating under an injection pressure of 1200bar. The operating conditions are summarized in Table 1. The physical properties of this fuel-model (mixture of 70% vol n-decane and 30% vol 1-methylnaphthalene) have been generated by the *ReFGen* software [31]. One may also found in Table 2 the different parameters of the calculations, including the DVI model parameters. Four test cases are defined in Table 3. As the injection boundary conditions are not fully known, some of them have been investigated numerically. In the following, Case 1 will be considered as the reference case. Particularly, it employs the experimental flow rate shown in Figure 5 and a liquid volume fraction,  $\alpha_l = 0.85$  at the hole exit. The case 2 uses a modified flat flow rate during the full opening period, also shown in Figure 5. Then, case 3 uses a value of  $\alpha_l$  equal to 0.80 in order to study the effects of cavitation in the orifice on the jet. Finally, case 4 employs the SGS dynamic Smagorinsky model instead of the standard Smagorinsky model used in the first three cases. For each case, a series of 15 or 30 LES was calculated by setting different seeds for random sampling of the injected blobs. In addition, the LES computations have been carried out with a well refined mesh in the injection zone (Figure 3). The characteristic size of the tetrahedral cells is of the order of 80 microns over a distance of about 100 diameters from the nozzle

exit. This mesh refinement aims at resolving the Gaussian profiles of liquid volume fraction and velocity specified by the DVI model.

### Case 1 results and discussion

The results of Case 1 are discussed using Figure 6 to Figure 9. First, the structure of the jet is shown in Figure 6 by presenting together the vapor fuel density distribution and the droplets distribution in the time range between  $t = 0.1$  and  $0.5$  ms. First, for  $t < 0.2$ ms, the liquid and vapor jets are superposed. Then, the vapor is driven by the leading gas eddies of the jet while the liquid spray keeps its penetration almost constant before evaporating completely towards  $0.5$  ms. At that moment, the structure of the jet obtained by LES is similar to the experimental snapshots as shown in Figure 7. It may be noted the presence of oscillations in the tail of the jet similar to those that can be observed on the experimental images. These oscillations seem to be originating from the DVI region (Figure 6). Hence, the turbulence intensity specified by  $V_{rms} = 0.2$  (see Equation(5)) and the one generated by the Gaussian velocity profile seem having played an essential role in the destabilization and the development of vortices around the DVI region. Figure 8(a) and (b) compares the fuel mass density obtained by averaging 50 experimental successive injections with the image obtained by averaging 30 LES calculations. A good correspondence between the calculated and measured jets can be noticed. The iso-values of fuel mass density are similar but their shapes are less regular than in the experimental image. This shows the need to carry out more than 30 computations in order to obtain more accurate comparisons. Figure 8(c) and (d) compares the numerical and experimental root mean square (RMS) of the fuel mass density (referred to as RO\_FUEL\_rms). It can be seen an overestimation in the calculations by almost 30% of RO\_FUEL\_rms. The reason of this result is not fully understood. In fact, both numerical and experimental results need to be verified in order to find the origin this disagreement. Axial and radial profiles of fuel density of 30 LES computations are represented in Figure 9. Their average shows good agreement with experimental profile (average of 50 injections). However, the oscillations of the calculated average axial profile persist, showing again the need to carry out more than 30 LES simulations. Radial profiles of fuel density are shown in Figure 9 for a distance from injector (Zprof) equal to 30 mm. Eight numerical radial profiles were extracted every  $45^\circ$  from the 3D jet results, in order to improve the statistics in the radial direction. The average of these (8 times 30) profiles shows very good agreement with experiments (average of 50 injections).

### Sensitivity study results and discussion

The sensitivity study is based on the five test cases defined in Table 3. The analysis of the LES results is based on the comparison of the radial profiles of the fuel mass density at  $0.5$  ms illustrated in Figure 10.

The influence of the turbulent SGS model is based on the comparison of Case 1 (using the Smagorinsky model, subsequently referred to as SMAGO) vs. Case 4 (using the dynamic Smagorinsky model, subsequently referred to as SMAGO\_DYN). A priori, the selective nature of the SMAGO\_DYN model is preferable; however the radial density profiles obtained by the SMAGO model are closer to the experimental results (Figure 10). This result shows that the use of the SMAGO model with a very refined mesh may be a good combination for internal combustion engine LES. Next, the influence of the number of LES computations is investigated using Case 1. As discussed in the previous section, the averaging of 30 injection computations instead of 15 improves the statistics results. However, it is worth to note on Figure 10 that the radial profiles are very similar using 15 and 30 computations. Indeed, as eight radial profiles are extracted from the computations at each jet section, the averages are made with a total of 120 and 240 profiles, respectively. This makes the numerical statistics in the radial direction very accurate. The influence of the rate of injection (ROI) shape shown in Figure 5 is highlighted by the comparison of Case 1 and Case 2. In particular, the value of the averaged density in case 2 is lower than in Case 1. This seems to show that very accurate ROI is necessary in order to capture transient injection phenomena.

Finally, the comparison of Case 1 with Case 3 allows studying the effects of the cavitation on the fuel jet although cavitation cannot be seen only by a reduction of area of the hole. Indeed, it is well known that the presence of cavitation in injection holes leads to a significant change in the fluid flow features. One of the parameters which undergo a significant modification is the liquid volume fraction,  $\alpha_l$ . Hence,  $\alpha_l$  has been changed from 0.85 in case 1 to 0.80 in case 3 (see Table 3). Although this variation of  $\alpha_l$  is weak, Figure 10 shows important changes between the two case results in terms of radial profiles of averaged mass density. Therefore, the computation of the cavitating flow in the orifices of diesel injectors seems essential in order to improve the numerical results of liquid jets.

### Summary and Conclusions

A new injection model called DVI (as Dense Volume Injection) model has been suggested in this work in order to improve the numerical results of Diesel liquid jets. This model specifies the main two-phase flow features in the DVI-region, in terms of volume fraction, velocity and turbulence for both liquid and gas phases. In parallel, a specific experiment has been performed in order to validate the two-phase flow models in the AVBP software and especially the DVI model. Two dimensional fields of instantaneous fuel mass concentration in the

jet were obtained by normalized Laser Induced Fluorescence where a normalization method based on the determination of the total injected mass was used to derive quantitative information from the fluorescence imaging.

The LES simulations have been carried out with a well refined mesh in the injection zone. In particular, this mesh correctly resolves the Gaussian profiles of liquid volume fraction and velocity specified by the DVI model.

Five test cases were computed. For each case, a series of 15 or 30 LES was calculated. From this numerical investigation, the following conclusions have been drawn:

- It is possible to obtain a satisfactory quantitative agreement between the numerical results and the experiments using the DVI model along with the correct upstream boundary conditions (such as the ROI, the turbulence level, the effective orifice section due to cavitation, the initial cone angle ...).
- A characteristic size of cells of the order of 80 microns seems to be small enough for resolving the liquid volume fraction and velocity profiles close to the nozzle exit.
- It has been shown that more than 30 LES simulations are needed in order to obtain converged LES results.
- For the LES SGS modeling, it seems that the use of the standard Smagorinsky model with a very refined mesh may be a good combination for internal combustion engine LES.
- This work also shows that two-phase flows and LES are already ready to be used in configurations of interest for the industry.

In the future, the computation of the cavitating flow in the orifices of diesel injectors seems essential in order to reduce the number of unknown boundary conditions and to improve the numerical results of Diesel engine simulations.

### Acknowledgements

The numerical work has been supported by the French ANR agency in the framework of the project SIGLE (ANR-07-PDIT-002). The experimental work has been supported by the GSM (PSA, Renault and IFPEN). The authors thank Mr. A. Robert (PhD student at IFPEN) for providing the grid used in this article.

### References

- [1] Y. Yue, C. F. Powell, R. Poola, J. Wang, and J. K. Schaller, "Quantitative measurements of diesel fuel spray characteristics in the near-nozzle region using x-ray absorption," *Atomization and Sprays*, vol. 11, no. 4, pp. 471–490, 2001.
- [2] P. Marmottant and E. Villermaux, "On spray formation," *Journal of Fluid Mechanics*, vol. 498, pp. 73–111, 2004.
- [3] M. Herrmann, "On simulating primary atomization using the refined level set grid method," *Atomization and Sprays*, vol. 21, no. 4, pp. 283–301, 2011.
- [4] E. d. Villiers, A. D. Gosman, and H. G. Weller, "Large Eddy Simulation of Primary Diesel Spray Atomization," *SAE Paper 2004-01-0100*, 2004.
- [5] O. Desjardins, V. Moureau, and H. Pitsch, "An accurate conservative level set/ghost fluid method for simulating turbulent atomization," *Journal of Computational Physics*, vol. 227, no. 18, pp. 8395 – 8416, 2008.
- [6] R. Lebas, T. Menard, P. Beau, A. Berlemont, and F. Demoulin, "Numerical simulation of primary break-up and atomization: DNS and modelling study," *International Journal of Multiphase Flow*, vol. 35, no. 3, pp. 247 – 260, 2009.
- [7] J. Shinjo and A. Umemura, "Surface instability and primary atomization characteristics of straight liquid jet sprays," *International Journal of Multiphase Flow*, vol. 37, no. 10, pp. 1294 – 1304, 2011.
- [8] A. Vallet, A. Burluka, and R. Borghi, "Development of a Eulerian Model for the "Atomization" of a Liquid Jet," *Atomization and Sprays*, vol. 11, pp. 619–642, 2001.
- [9] V. Iyer and J. Abraham, "Two-fluid modeling of spray penetration and dispersion under Diesel engine conditions," *Atomization and Sprays*, vol. 15, pp. 249–269, 2005.
- [10] B. M. Devassy, C. Habchi, and E. Daniel, "Numerical investigation of Eulerian Atomization Models based on a Diffuse-Interface two-phase flow approach coupled with surface density equation," in *ILASS-Europe, 24th European Conference on Liquid Atomization and Spray Systems, Estoril, Portugal*, 2011.
- [11] R. Reitz, "Modeling atomization processes in high-pressure vaporizing sprays," *Atomisation and Spray Technology*, vol. 3, pp. 309–337, 1987.
- [12] K. Huh and A. Gosman, "A phenomenological Model for Diesel Spray Atomization." Tsukuba, Japan: International Conference On Multiphase Flows'91, 24-27 September 1991.
- [13] C. Habchi, D. Verhoeven, C. H. Huu, L. Lambert, J. L. Vanhemelryck, and T. Baritaud, "Modeling Atomization and Break Up in High-Pressure Diesel Sprays," *SAE Paper 970881*, 1997.
- [14] F. Tanner and G. Weisser, "Simulation of liquid jet atomization for fuel sprays by means of a cascade drop breakup model," *SAE Paper 980808*, 1998.
- [15] G. Bianchi, P. Pelloni, F. Corcione, L. Allocca, and L. F., "Modeling Atomization of High Pressure Diesel Sprays," *ASME Journal of Engineering for Gas Turbines and Power*, 2001.
- [16] J. Abraham and L. M. Pickett, "Computed and measured fuel vapor distribution in a diesel spray," *Atomization and Sprays*, vol. 20, no. 3, pp. 241–250, 2010.
- [17] J. Abraham, "What Is Adequate Resolution in the Numerical Computations of Transient Jets?" *Trans. of the SAE*, vol. 106, pp. 141–155, 1997.
- [18] J. Abraham and V. Magi, "A Virtual Liquid Source (VLS) model for vaporizing Diesel sprays," *SAE Paper 1999-01-0911*, 1999.
- [19] L. Martinez, A. Benkenida, and B. Cuenot, "A model for the injection boundary conditions in the context of 3D simulation of Diesel Spray: Methodology and validation," *Fuel*, vol. 89, no. 1, pp. 219 – 228, 2010.

- [20] M. Sanjosé, J. Senoner, F. Jaegle, B. Cuenot, S. Moreau, and T. Poinso, “Fuel injection model for Euler-Euler and Euler-Lagrange large-eddy simulations of an evaporating spray inside an aeronautical combustor,” *International Journal of Multiphase Flow*, vol. 37, no. 5, pp. 514 – 529, 2011.
- [21] O. Simonin, L. Zaichik, V. Alipchenkov, and P. Février, “Connection between two statistical approaches for the modelling of particle velocity and concentration distributions in turbulent flow: The mesoscopic Eulerian formalism and the two-point probability density function method,” *Physics of Fluids*, vol. 18, p. 125107, 2006.
- [22] G. Bruneaux, “Study of the Effect of Wall Guiding on Direct Diesel Injection by Optical Diagnostics,” in *The Seventh International Conference on Modeling and Diagnostics for Advanced Engine Systems (COMODIA)*, Japan, 2008, pp. 585–592.
- [23] G. Bruneaux and D.Maligne, “Study of the mixing and Combustion Processes of Consecutive Short Double Diesel Injections,” *SAE paper*, 2009.
- [24] H. Chaves, C. Kirmse, and F. Obermeier, “Velocity measurement of dense diesel fuel sprays in dense air,” *Atomization and Sprays*, vol. 14, pp. 589–609, 2004.
- [25] D. Siebers, “Ignition delay characteristics of alternative diesel fuels: Implications on cetane number,” S. International, Ed., no. SAE paper 852102, 1985.
- [26] D. Verhoeven, J. Vanhemelryck, and T. Baritaud, “Macroscopic and ignition characteristics of high-pressure sprays of single-component fuels,” *SAE Paper 981069*, 1998.
- [27] G. Bruneaux, “Liquid and Vapor Spray Structure in High Pressure Common Rail Diesel Injector,” *Atomization and Sprays*, vol. 11, pp. 553–556, 2001.
- [28] G. Bruneaux, “Mixing Process in High Pressure Diesel Jets by Normalized Laser Induced Exciplex Fluorescence. Part I: Free Jet,” *SAE Transactions*, vol. 114, no. 3, pp. 1444–1461, 2005.
- [29] E. Riber, V. Moureau, M. García, T. Poinso, and O. Simonin, “Evaluation of numerical strategies for large eddy simulation of particulate two-phase recirculating flows,” *Journal of Computational Physics*, vol. 228, no. 2, pp. 539 – 564, 2009.
- [30] C. Habchi, “The energy Spectrum Analogy Breakup (SAB) model for the numerical simulation of sprays,” *Atomization and Sprays*, vol. 21, no. 12, pp. 1033–1057, 2011.
- [31] R. Lugo, V. Ebrahimian, C. Lefebvre, C. Habchi, and J.-C. de Hemptinne, “A compositional representative fuel model for biofuels - application to diesel engine modelling,” no. SAE paper 2010-01-2183, 10 2010.

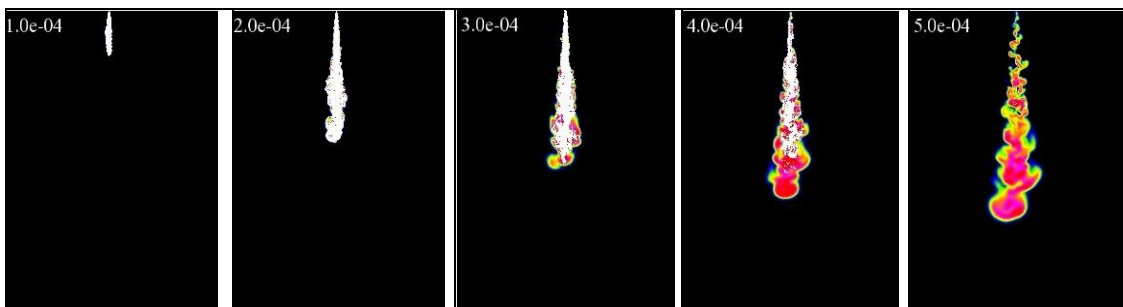
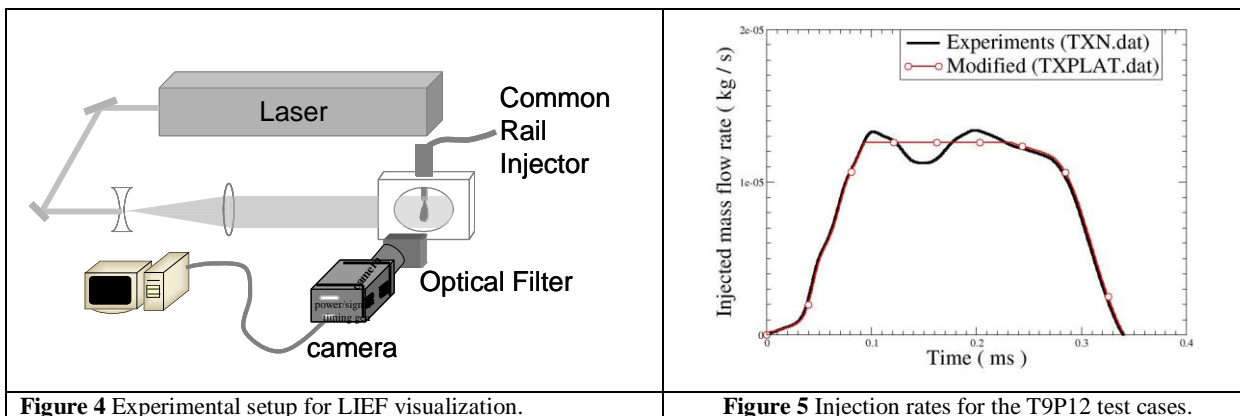
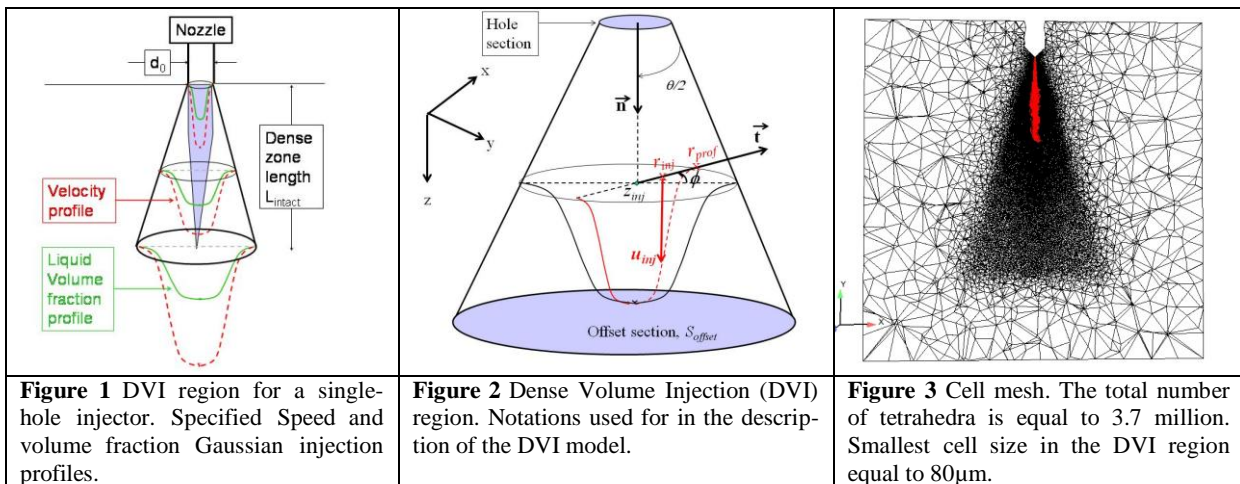
## Tables

Fuel model	70% vol n-decane + 30% vol 1-methylnaphtalene	mix7030 obtained by <i>ReFGen</i> software [31].
Injection pressure	bar	1200
Gas mass density	kg/m <sup>3</sup>	25
Gas pressure	bar	67
Gas temperature	K	900
Initial fuel temperature	K	348

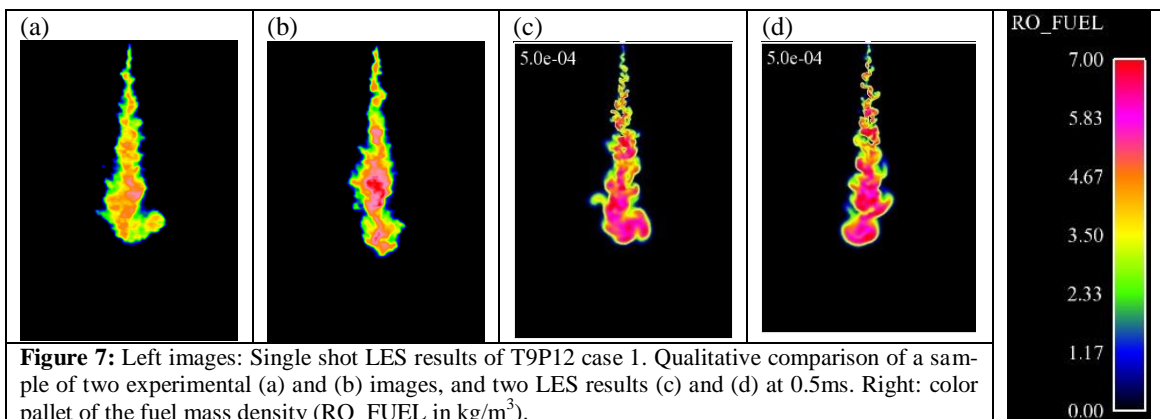
Hole diameter	$d_o$	μm	200
Cone angle	$\theta$	°	20
Cone angle fluctuation	$\theta'$	°	1
Dense liquid core length	$L_{intact}$	mm	2
Velocity Discharge coefficient	$Cd_{vit}$	-	1.0
Liquid volume fraction in the injector orifice	$\alpha_l$	-	0.8 and 0.85
Intensity of the initial velocity fluctuation	$V_{rms}$	-	0.2
Entrainment factor	$F_{glis}$	-	0.3
Injection duration	$T_{ini}$	μs	340
Opening and closing durations	dtopen, dtclose	μs	0 , 40
Blobs characteristic size distribution	Rosin-Rammler	-	SMD = 5 μm and qrr=3.5
Total number of injected parcels	tncparc	-	50000
Total injected mass	tspmas	mg	2.45
Injection rate	$M_{dot}$	Figure 5	Labels TXN and TXPLAT

Case	Label	Injection rate (Figure 5)	$\alpha_l$	SGS models	Total number of LES
1(15)	A85	TXN	0.85	Smagorinsky model	15
1(30)					30
2(15)	TXE	TXPLAT	0.85	Smagorinsky model	15
3(15)	TXN	TXN	0.8	Smagorinsky model	15
4(30)	DYN	TXN	0.85	Dynamic Smagorinsky model	30

Figures



**Figure 6** Single shot LES results of T9P12 case 1 – Superposition of the distribution of the fuel mass density and the liquid spray (in white).





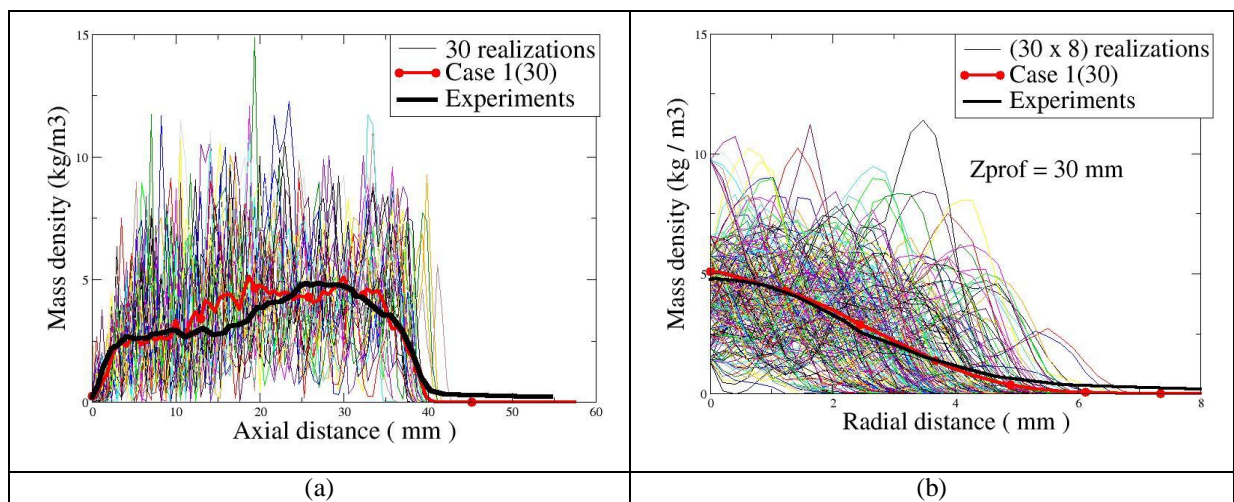
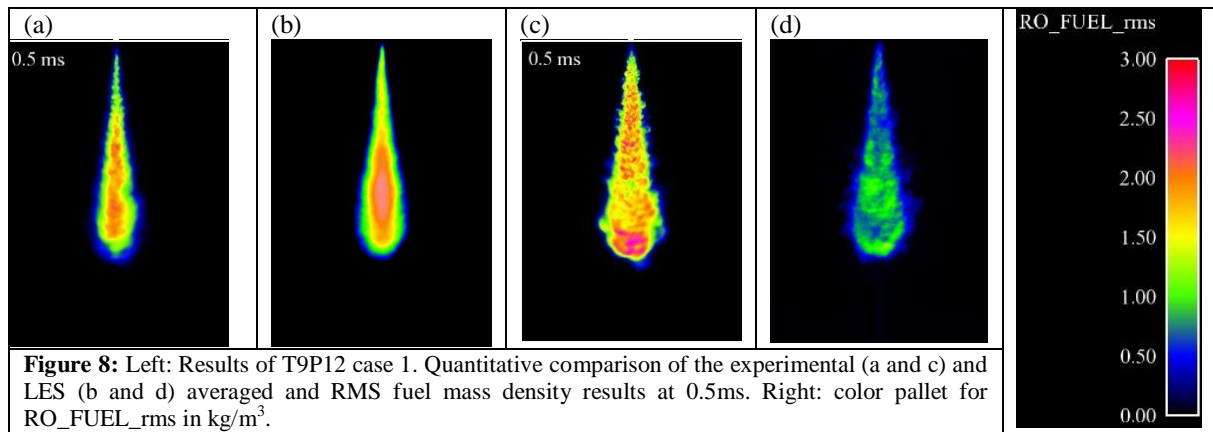


**Figure 9** Results of T9P12 case 1. Comparison of the experimental and LES centerline, (a), and radial profiles (b) of the fuel mass density at time  $t=0.5\text{ms}$ . The axial locations of radial profiles is  $Z_{\text{prof}}=30\text{mm}$  from the nozzle exit. The red curve with solid circles is the average of 30 LES profiles depicted by thin lines.

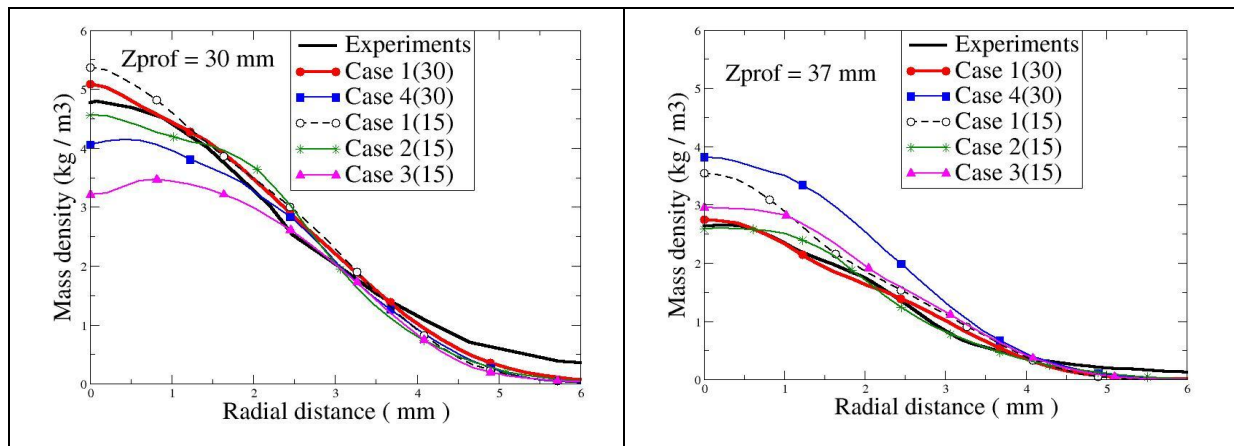


**Figure 10** Comparison of the experimental and LES radial profiles of the fuel mass density at  $t=0.5\text{ms}$  for the different test case defined in Table 3. Influence of the SGS model (Case 1 vs 4). Number of LES computations (Case 1(30) vs. Case 1(15)). Injection rate shape (Case 1 vs. 2). Cavitation (Case 1 vs. 3).